JMEPEG
https://doi.org/10.1007/s11665-025-11499-6
©The Author(s)
1059-9495/$19.00

ORIGINAL RESEARCH ARTICLE

Generalized Failure Criteria for Computational Modeling of Dynamic Failure

Elena Sitnikova

Submitted: 22 December 2024 / Revised: 27 March 2025 / Accepted: 25 April 2025

In the present paper, a framework for defining the dynamic failure of materials at a general stress state is developed. Method of extending conventional quasi-static failure criteria into their dynamic formulation is proposed that utilizes a concept of incubation time of failure. The incubation time property has been previously employed in formulating the dynamic failure condition that offers a more physically meaningful and robust alternative to popular dynamic failure prediction methods involving strain rate dependency of the strength of the material. Making use of the appropriately defined incubation times and stress invariants that are commonly involved in formulation of the quasi-static failure criteria, their dynamic counterparts can be delivered. The generalization has been carried out for three popular failure criteria. Challenges of generalizing the incubation time-based criterion to arbitrary load histories have been discussed, and a method of implementing it in such cases has been presented.

Keywords dynamic loading, failure analysis, failure criteria, modeling and simulation

1. Introduction

When addressing problem of the dynamic failure of materials, it is a commonplace practice to involve a so-called dynamic strength of the material as a material property, that is considered as a function of the strain rate. This approach largely owes its popularity to Johnson-Cook dynamic plasticity and failure model (Ref 1) that has been implemented in leading finite element (FE) solvers, such as Abaqus (Ref 2), and is currently the most popular computational modeling tool for predicting the dynamic failure of isotropic materials.

Effectively, in such failure criteria, the dynamic failure is treated as an instantaneous event, when the failure takes place as soon as the stress, σ, in the material reaches a critical value, σ_d, i.e.,

$$\sigma < \sigma_d, \tag{Eq 1}$$

This criterion in its form is identical to a quasi-static maximum stress criterion with the only exception that the dynamic strength is no longer a constant, but a property, which can be written in a general from as

$$\sigma_d = \sigma_d(a_1, a_2, .., \dot{\varepsilon}, T), \tag{Eq 2}$$

where $\dot{\varepsilon}$ is the strain rate, a_i are parameters of the criterion and variable T is the temperature, which is primarily involved in definition of dynamic behavior of metallic materials, for which such dependencies were originally proposed. The so-called rate dependency of strength has been captured experimentally on numerous occasions, e.g., (Ref 1, 3), and specific form of (2) is determined by fitting the experimental data, typically, with an exponential or a logarithmic function.

Despite their vast popularity, being empirical in their nature, the strain-rate-based dynamic failure criteria suffer a number of critical drawbacks. The obvious problem is lack of clear physical meaning of parameters involved in definition of these criteria, since these are introduced merely as fitting coefficients. Furthermore, the fitting is primarily applied to data obtained at high strain rates and as such, it does not cover the entire range of the strain rates. Consider the Johnson-Cook dynamic yield limit (Ref 4)

$$\sigma_d = [A + B(\bar{\varepsilon}^{pl})^n]\left[1 + C\ln\left(\frac{\dot{\bar{\varepsilon}}^{pl}}{\dot{\varepsilon}_0}\right)\right](1 - T^{*m}). \tag{Eq 3}$$

where σ_d is the dynamic strength of the material, $\bar{\varepsilon}^{pl}$ is the equivalent plastic strain, $\dot{\bar{\varepsilon}}^{pl}$ is the strain rate, A, B, C, n, m are the coefficients and T^* is the temperature function. A reduced form of this criterion,

$$\sigma_d(\dot{\varepsilon}) = \sigma_*\left[1 + C\ln\left(\frac{\dot{\varepsilon}}{\dot{\varepsilon}_0}\right)\right], \tag{Eq 4}$$

where σ^* is the quasi-static strength, was employed in (Ref 5) to define rate-dependency of the dynamic strength for a unidirectional composite material. While it was produced by fitting the experimental data, it can be viewed as a reduced version of the Johnson-Cook criterion for a case of uniaxial loading where no plastic flow or temperature variations take

This article is an invited paper selected from presentations at the 5th International Symposium on Dynamic Response and Failure of Composite Materials, held June 17-21, 2024, in Island of Ischia, Italy, organized by Prof. Valentina Lopresto, Dr. Ilaria Papa, Prof. Michele Guida, and Prof. Antonello Astarita, University of Naples Federico II. It has been expanded from the first presentation and peer reviewed as an original paper following the standard procedure of the journal.

Elena Sitnikova, Department of Mechanical Engineering, School of Engineering, University of Southampton, Southampton SO17 1BJ, UK. Contact e-mail: elena.sitnikova@soton.ac.uk.

Published online: 16 June 2025

place. It uses two fitting coefficients, C and $\dot{\varepsilon}_0$, the latter of which is referred to as the 'reference strain rate.' Effectively, it is a cutoff strain rate below which the material failure response is assumed to be static. Fitting it to rate dependence of the dynamic strength of Gurit 20LV epoxy resin (Ref 6) as was captured experimentally in (Ref 7), the curve as shown in Fig. 1(a) is obtained. The values of the material properties were $E = 3.5$GPa for Young's modulus, $\nu = 0.35$ for Poisson ratio and $\sigma_* = 75$MPa for the quasi-static strength. As can be seen, the dynamic strength dependence on strain rate is not even smooth, being maintained at its quasi-static value while $\dot{\varepsilon} < \dot{\varepsilon}_0$ and increasing sharply beyond this point.

Another consideration against use of strain-rate based approaches is that to define the rate dependency of dynamic strength through curve fitting, the latter should be measured at constant strain rates. Ensuring constancy of strain rate can itself be a challenging task, and additional measures need to be taken to achieve this in the experiments, especially when testing brittle materials (Ref 8). However, constancy of the strain rate is by no means guaranteed in real-life applications, where the time histories of the loads acting on the material can be very complex. Therefore, the applicability of such criteria for predicting failure in loading scenarios where the strain rate is not constant is rather questionable. Furthermore, the strain rate dependence of the dynamic strength is measured under uniaxial loading, and there is clear lack of understanding of how this can be extended to general loading scenario, where multiple stress components are nonzero. In Johnson-Cook criterion, an attempt was made to address the issue of generalization by adopting the effective stresses and strains in its formulation. While this can be considered as a pragmatic approach to generalization for isotropic materials, such as metals, for which this criterion was originally proposed, this method will certainly not be appropriate for many modern anisotropic materials, such as composites, that have strong directional dependency of the mechanical properties.

2. Incubation Time Concept and the Failure Criterion

An alternative methodology for addressing the dynamic failure problem has been proposed by Petrov (Ref 9-11). Its main underlying consideration is that the macroscopic experimentally observable fracture is a non-instantaneous event. It results from microscopic preparatory processes such as microcracking, interaction of pores and defects, that evolve over a certain time duration. The time duration associated with such processes has been referred to as the incubation time of failure, and it is treated as a material property reflecting the dynamic characteristics of the failure process. In case of high loading rates, the incubation time of failure is comparable to the duration of the load applied.

To reflect the dynamic nature of failure process, the dynamic criterion is defined in terms of the stress impulse rather than the stress itself. The expression of the incubation time criterion has been proposed as (Ref 9)

$$I_{\Im}(t_*) = \sigma_* \Im, \tag{Eq 5}$$

where σ_* is the quasi-static strength of the material, t_* is time to failure and is $\Im$ incubation time of failure. The stress impulse is calculated as

$$I_{\Im}(t) = \int_{t-\Im}^{t} \sigma(s)ds. \tag{Eq 6}$$

Note that the impulse is calculated over the time interval $\Im$, which does not have to coincide with the duration of the load applied. This signifies that according to criterion (5), the failure takes place when the stress impulse acting on the material over time $\Im$ reaches critical value.

Given that in dynamic testing of materials, such as split-Hopkinson bar tests, the results are often presented in terms of a strength as a function of the strain rate, it is helpful to obtain an analytical expression for such dependency based on the incubation time criterion (5). This will serve two purposes: demonstrate of the capability of the incubation time criterion in obtaining the analytical expression for the dynamic strength and facilitate determining the value of the incubation time. Analytical expression of strength as function of strain rate has been obtained in (Ref 12), where stress was considered as a function of strain rate as follows:

$$\sigma(t) = E\dot{\varepsilon}tH(t), \tag{Eq 7}$$

where $\sigma(t)$ is the stress as a function of time, E is the Young's modulus, $\dot{\varepsilon}$ is the constant strain rate and $H(t)$ is the Heaviside step function. Substituting (7) into (5) and carrying out necessary mathematical manipulations, as detailed in (Ref 12), one arrives at the expression of dynamic strength as a function of the strain rate as

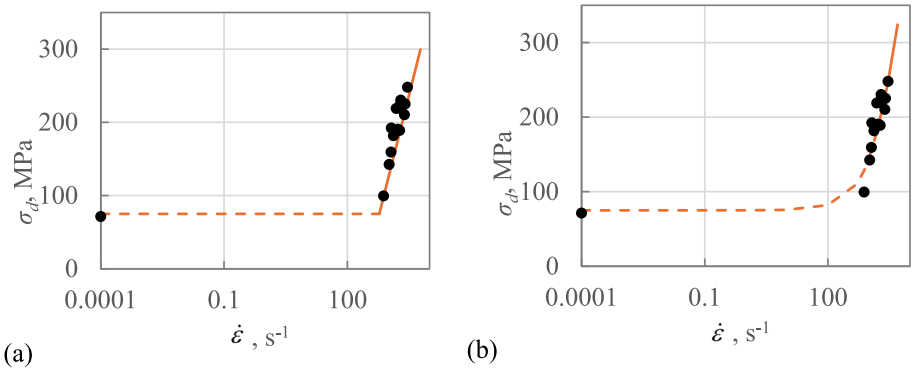

Fig. 1 Split-Hopkinson pressure bar (SHPB) test data for GURIT Prime 20 LV epoxy resin from (Ref 7) fitted with (a) logarithmic dependence (4) where $C = 1.3$, $\dot{\varepsilon}_0 = 600$ s^{-1}, (b) dynamic strength given by Eq 8 as derived from the incubation time criterion

$$\sigma_d(\dot{\varepsilon}) = \begin{cases} 2\sigma_* \sqrt{\frac{\dot{\varepsilon}}{\dot{\varepsilon}_s}}, & \dot{\varepsilon} \geq \dot{\varepsilon}_s \\ \sigma_* \left(1 + \frac{\dot{\varepsilon}}{\dot{\varepsilon}_s}\right), & \dot{\varepsilon} < \dot{\varepsilon}_s \end{cases} \qquad \dot{\varepsilon}_s = \frac{2\sigma_*}{E\Im}. \tag{Eq 8}$$

Two expressions in the right hand side of Eq (8) were obtained considering two possible failure scenarios: one where time at failure $t_* \leq \Im$, which is typical at high loading rates, and another where $t_* > \Im$, which corresponds to cases where load is of longer duration and lower amplitude. The expression for the reference strain rate $\dot{\varepsilon}_s$ has been obtained in (Ref 12) as a by-product of mathematical manipulations when deriving Eq 8. Having derived analytical expression of the dynamic strength, one can obtain the incubation time by fitting Eq 8 to the experimental data. Specifically, fitting Eq 8 to experimental dynamic strength data of the epoxy resin as shown in Fig. 1(b), the incubation time is obtained as $\Im = 40$ μs. Effectively, data from SHPB tests are a dynamic counterpart to quasi-static data obtained from the conventional coupon testing. Like the latter are used to determine the material properties associated with the quasi-static response, SHPB testing is adopted to determine the material properties associated with the dynamic behavior, which is the incubation time of failure. If the loading pulses in the tests are of a reasonably simple shape, expression of the dynamic strength can always be derived and fitted to the experimental data, through which the value of incubation time is determined, as is shown in the example above.

The main implication of the incubation time criterion, and its main conceptual difference from the approach based on the strain rate dependency of the dynamic strength is that the dynamic strength of the material is not viewed as a pre-determined material property, but it is a calculated characteristic that can vary depending on the loading history.

Incubation time approach has been extensively applied and developed by its authors to reproduce and explain various aspects of the dynamic behavior of materials (Ref 13, 14). Such studies predominantly involve finding analytical solutions for failure scenarios where loading pulses of simple shapes were producing uniaxial stress wave. This is dictated, on the one hand, by the complexity of deriving analytical solution under 2D or 3D stress states, but this also reflects the inherent limitation of the dynamic testing of materials, where stress and strain states can only be obtained under the uniaxial loading (Ref 15).

While studies of this kind enhance understanding of the dynamic failure process, they are insufficient for describing failure in practical scenarios, where multiple stresses are acting on the material, and their time histories can be completely arbitrary. Extending the method to brittle materials, one would need to take into consideration that the tensile strength for brittle materials can be significantly smaller than its counterpart under compression. The problem is further exacerbated for advanced materials, such as composites, by the directional dependency of their mechanical properties. Furthermore, most quasi-static failure criteria account for interaction between different stress components that makes a profound difference on failure predictions, and this must also be reflected in the dynamic failure criteria.

With development of modern FE solvers, that are powerful computational tools for stress analysis under the arbitrary dynamic loading, the demand for reliable and robust dynamic failure criteria capable for failure predictions under the general stress state is more acute than ever. To address this demand, generalization principle for the incubation time criterion will be proposed in the present paper as the first step in this direction.

3. Generalization of the Incubation Time Criterion

3.1 Arbitrary Loading History

Finite element solvers provide stress time histories as a standard output of the analysis. The calculation of the total stress impulse is therefore straightforward; all one needs to do is to calculate as the area under the stress curve using trapezoidal rule of integration:

$$I_{\Im}(t) = \int_0^t \sigma(s)ds = \sum_{i=1}^{n} \frac{\sigma_i + \sigma_{i-1}}{2} \Delta t_i \tag{Eq 9}$$

where Δt_i is the time increment, σ_{i-1} and σ_i are stresses at the beginning and the end of the time increment and n is the number of time increments. This readily delivers a value of the impulse to be checked against the critical impulse in failure scenarios where material is expected to fail at times $t_* \leq \Im$.

The difficulty in implementation of the incubation time criterion arises when one needs to calculate impulse in (6) over the time interval $\Im$ when $t_* > \Im$. To do so, effectively, one needs to shift the 'window' of integration along the time axis at each time increment, as is schematically shown in Fig. 2(a), so that the integration is always performed over the time interval $\Im$. In general, at any time instance, impulse over the integration interval $\Im$, $I_{\Im}(t)$, can be calculated as

$$I_{\Im}(t) = I(t) - I(t - \Im). \tag{Eq 10}$$

Calculation of $I(t)$, which is a total impulse over the entire stress history, is readily given by Eq 9. The main technical challenge is calculation of $I(t - \Im)$, because, when writing a user-defined material subroutine, the user only has access to the current value of stress, value of stress at previous increment and the current time increment. Storing stress values over the entire time interval $\Im$ would not be a practical option, because in full-scale simulations of the dynamic failure of parts and components, time increments could be several orders of magnitude smaller than the incubation time $\Im$. It is apparent that storing and updating the respective values of the impulse increments would be very computationally costly.

More efficient alternative to calculating the impulse over the integration interval $\Im$ is to use a linear approximation. The schematic of the procedure is shown in Fig. 2(b). At any time increment, the total impulse at current and the previous time increments, $I(t)$ and $I(t - \Delta t)$, respectively, are calculated directly using Eq 9. The total impulse $I(t - \Im)$ can be obtained assuming linear approximation of total impulse locally. Using this assumption, its explicit expression has been derived as

$$I(t - \Im) = \frac{I(t - \Delta t)\Delta t - I(t - \Delta t - \Im)(2t - \Im - \Delta t)}{\Im}, \tag{Eq 11}$$

where $I(t - \Im - \Delta t)$ is the value of $I(t - \Im)$ at the previous time increment. It is zero initially and is assigned an approximate value of $I(t - \Im)$ at the end of each time increment when $t > \Im + \Delta t$.

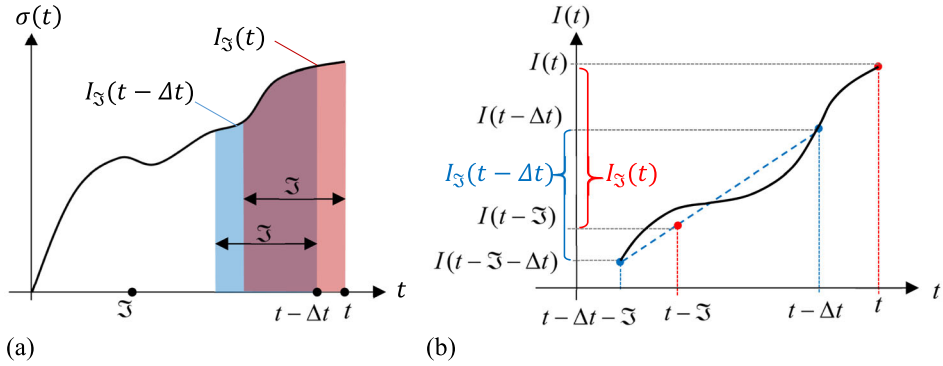

Fig. 2 Impulse over the integration interval ϑ: (a) visualization of the concept; (b) linear fitting of the total impulse

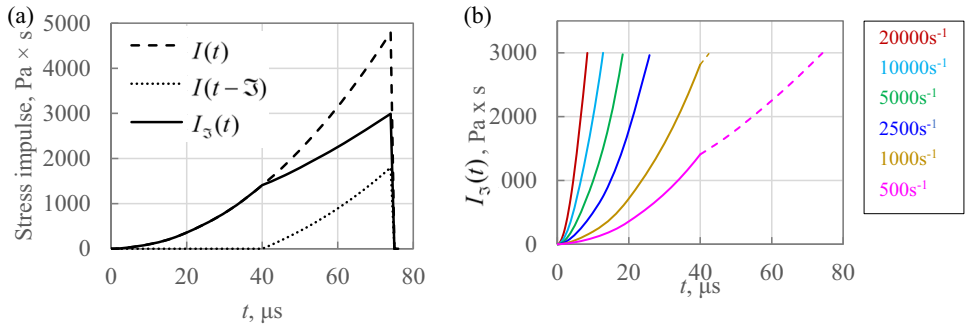

Fig. 3 Calculation of the impulse stress: (a) stress impulse components as involved in Eq 10 (b) time histories of $I_\vartheta(t)$ at different strain rates

The incubation time criterion (5) has been implemented as a user-defined VUMAT material subroutine in Abaqus, and the implementation included the procedure for calculating the impulse over time interval ϑ based on approximate method as described above. The implementation of the code has been verified using a single element model generated in Abaqus/Explicit. Cubic C3D8R element had dimensions 10 mm × 10 mm × 10 mm. The material properties were those of Gurit 20LV epoxy resin (Ref 6), including the incubation time $\vartheta = 40$ μs that was determined in the previous section. The material density, which is an essential input parameter in dynamic simulations, was specified as 1400 kg/m^3. The boundary conditions were applied to the model in terms of relative displacements (Ref 16), so that the single element would represent a unit cell for the isotropic material. The so-called key degrees of freedom (KDoFs), as described in (Ref 16), are crucial in definition and implementation of the relative displacement boundary conditions, and they offer very convenient means of applying the load. It is worth noting that to date there has been no systematic exploration of the how the unit cell boundary conditions should be used in dynamic problems. Nevertheless, for the purpose of the present exercise, using KDoFs as means of prescribing the load allowed achieving uniform loading with constant strain rate. For that, displacement was applied at one KDoF monotonically as a ramp function. By varying the applied displacement values and time durations, different strain rates have been obtained.

Typical time histories of the impulses as involved in Eq 10 are shown in Figure 3(a). The total impulse, $I(t)$, continuously increases up to the moment of failure, as one would expect. The time history of the impulse over the incubation time interval $\vartheta = 40$ μs, $I_\vartheta(t)$, coincides with that of $I(t)$ while $t \le \vartheta$, which is also to be expected. At $t = \vartheta$, a kink in plot of $I_\vartheta(t)$ can be observed, because at this point impulse $I(t - \vartheta)$ becomes nonzero. Since value of this impulse is not calculated precisely but based on a linear approximation, this, in turn, naturally affects accuracy in calculating $I_\vartheta(t)$ when $t > \vartheta$. Note that in this case, as well as during loading at any other strain rate, the failure is predicted once $I_\vartheta(t) = 3000$Pa × s, as can be seen in Figure 3(b). This reproduces the value of critical impulse as defined in Eq 5, namely, $\sigma_* \vartheta = 75$MPa × 40μs.

As an additional verification, the values of stresses at failure predicted at different strain rates have been plotted against time to failure in Fig. 4(a). The plot reproduces classical appearance of the dynamic strength curve, where, as times to failure $t_* \to \infty$, it asymptotically approaches the quasi-static strength value, while as $t_* \to 0$, it rapidly increases. Time dependency of dynamic strength offers a more universal representation of this characteristic than presenting it merely as a function of strain rate, since it does not pose a restriction on the loading pulse in terms of constancy of the strain rate.

It is also informative to consider the stress-strain curves obtained at different strain rates. Stresses in the loading direction have been plotted as functions of strains in the same direction in Fig. 4(b). The stresses and strains were calculated up to failure. At strain rates of up to 1000 s^{-1}, the stress-strain dependency appears to be linear, while the higher the strain rate, the more deviation from linear appearance, and the steeper the slopes of the curves. Such 'stiffening' of the material at high strain rates is typical observation in the SHPB tests, e.g., in (Ref 17). The cause for loss of linearity in stress-strain curves is the material inertia. The effects of the inertia on the stress state are illustrated in Fig. 5, where time histories of stresses calculated at three different stain rates are presented. At low strain rates,

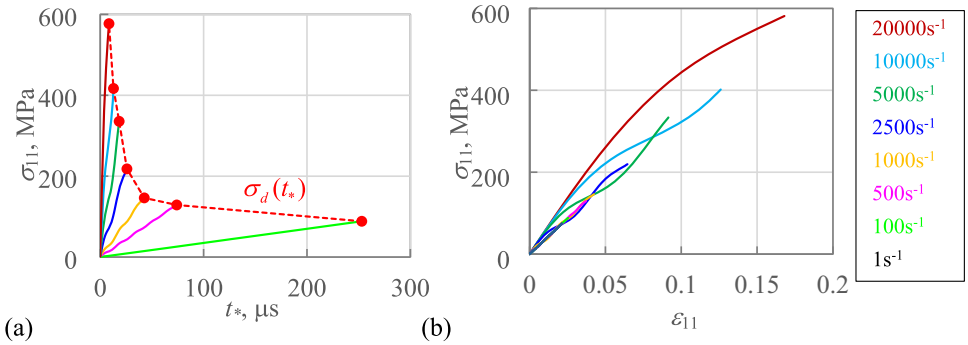

Fig. 4 (a) Dynamic strength corresponding to loading at constant strain rates as function of time to failure (b) Stress-strain curves at different strain rates

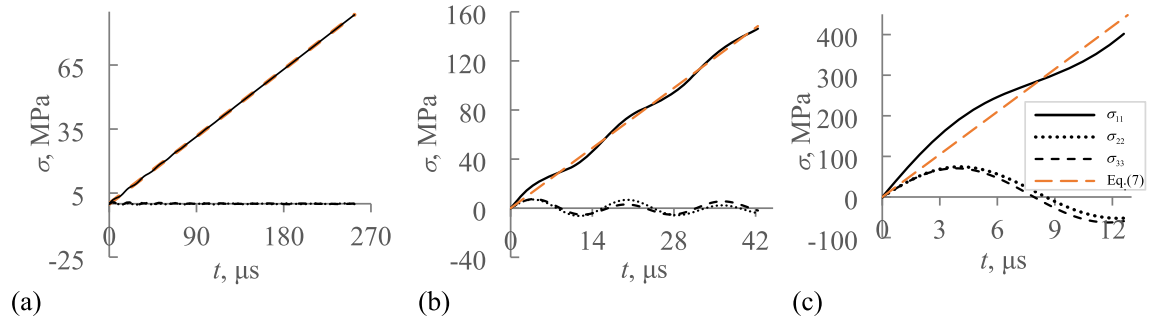

Fig. 5 Time histories of the direct stresses for loading at (a) $\dot{\varepsilon} = 100$ s^{-1}; (b) $\dot{\varepsilon} = 1000$ s^{-1} and (c) $\dot{\varepsilon} = 10000$ s^{-1}

the material is effectively under the uniaxial stress state, as shown in Fig. 5(a). Direct stress σ_{11} is in the direction of the applied load and it generally coincides with the stress at constant strain rate given by Eq 7, but it is not perfectly linear as it tends to slightly oscillate around the linear stress time history plot. Similarly, direct stresses σ_{22} and σ_{33} tend to oscillate around zero value, but their amplitudes are well below 1 MPa. Both tendencies become increasingly more pronounced at loads associated with high strain rates. As shown in Fig. 5(b), at 1000 s^{-1} the amplitudes of σ_{22} and σ_{33} increase up to 7 MPa and oscillations are also clearly seen in the time history of σ_{11}. At 10000 s^{-1}, the amplitudes of σ_{22} and σ_{33} become comparable to the quasi-static strength value, σ_*, and σ_{11} significantly deviates from its linear approximation given by Eq 7.

These results indicate that the loss of linearity in stress-strain curves and apparent increase is stiffness at high loading rates is due to inertia of the material. Abaqus/Explicit is capable of reproducing its effects without introducing any additional assumptions on material constitutive behavior. It is worth noting that in presence of other nonzero stress components, the slopes of the stress-stain curves at high strain rates in Fig. 4(b) do not actually represent the stiffness of the material, because stiffness must be defined under the uniaxial stress state.

While in the examples above only the loading cases delivering constant strain rates were considered, it is obvious that the applicability of the incubation time criterion is not limited to this type of loading, as the criterion itself is not restricted to any specific stress history. Note that due to the practical need to approximate the stress impulse, overall, it is best suited for analyzing loading cases where the stress changes reasonably monotonically, which may not be the case for all general loading conditions. However, the impulse approximation (11) begins to play part only for loads acting over longer time intervals, namely, $t > \tau$, while for loads of short duration and high amplitude the failure predictions are not affected by this approximation.

3.2 Concept of the Averaged Stress

It can easily be shown that criterion (5) is a dynamic counterpart of the classical maximum stress criterion. Introducing

$$\overline{\sigma}_\tau(t) = \frac{I_\tau(t)}{\tau} = \frac{\int_{t-\tau}^{t} \sigma(s)ds}{\tau} \qquad \text{(Eq 12)}$$

criterion (5) can be re-written as

$$\overline{\sigma}_\tau(t_*) = \sigma_*, \qquad \text{(Eq 13)}$$

where variable $\overline{\sigma}_\tau(t)$ is defined in Eq 12 as the stress impulse $I_\tau(t)$ averaged with respect to the incubation time. Since its units are Pascals, for brevity, it will be referred to as averaged stress. It is easy to see that Eq 13 is a maximum stress failure criterion expressed in terms of averaged stress. It is worth noting that the concept of dynamic stress intensity introduced in (Ref 18) effectively represents a stress impulse averaged over the incubation time with the only exception that the dynamics stress intensity from (Ref 18) also involves a shape parameter in the integrand. This parameter is of special relevance in dynamic plasticity problems, while the procedures for determining its value are not clearly defined. Plastic flow considerations would add the extra degree of complexity to generalization, therefore in the present paper, as a starting

point, failure is considered in a brittle sense, as a complete loss of load bearing capability once the critical condition is satisfied.

Implementation of this new formulation of the dynamic failure criterion requires very small change: all the impulses in formulation given in subsection 3.1 should be divided by the incubation time. This presentation of the criterion, in fact, significantly facilitates visualization and interpretation of the results. Consider time histories of the current stress and the averaged stress obtained at low and high strain rates in Fig. 6(a) and (b), respectively. As can be seen in Fig. 6(a), at slowly applied load, there is little difference between the two, and the current stress is only marginally higher than the averaged one. Failure is predicted once the averaged stress reaches the critical value. The latter is true universally, however, at high loading rate there is a significant discrepancy between the averaged and the current stress, as shown in Fig. 6(b), and at failure, the value of the current stress, $\sigma(t)$, is much higher than the value of the averaged stress, $\overline{\sigma}_{\Im}(t)$.

3.3 Generalization of Failure Criteria Based on Stress Invariants

Most of the phenomenological failure criteria are defined in terms of stress invariants, be it von Mises or Tresca criterion for the isotropic materials, or Tsai-Wu criterion for composites, to name a few. This offers common ground for generalizing the failure criteria to their dynamic counterparts. The concept of the averaged stress as introduced in the previous subsection can be extended to define the averaged stress invariant. Without loss of generality, consider von Mises yield criterion as an example:

$$\sigma_{\mathrm{v}} = \sqrt{3J_2} = \sigma_* \qquad \text{(Eq 14)}$$

where σ_{v} is the von Mises stress, σ_* is the tensile yield strength of the material, and J_2 is the second invariant of deviatoric stress tensor, expressed in terms of principal stresses as

$$J_2 = \frac{1}{6}\left[(\sigma_1-\sigma_2)^2 + (\sigma_2-\sigma_3)^2 + (\sigma_3-\sigma_1)^2\right]. \qquad \text{(Eq 15)}$$

Linearizing it, averaged von Mises stress becomes

$$\overline{\sigma}_{\mathrm{v}}(t) = \frac{1}{\Im}\int_{t-\Im}^{t} \sqrt{3J_2(s)}ds, \qquad \text{(Eq 16)}$$

which yields the dynamic generalization of von Mises criterion as follows:

$$\overline{\sigma}_{\mathrm{v}}(t_*) = \sigma_*. \qquad \text{(Eq 17)}$$

Similarly, generalized counterpart of Tresca failure criterion becomes

$$\frac{1}{\Im}\max\left(\int_{t_*-\Im}^{t_*}|\sigma_1(s)-\sigma_2(s)|ds, \int_{t_*-\Im}^{t_*}|\sigma_2(s)-\sigma_3(s)|ds, \int_{t_*-\Im}^{t_*}|\sigma_3(s)-\sigma_1(s)|ds\right) = \sigma_*. \qquad \text{(Eq 18)}$$

It is easy to see that if the load is applied uniaxially at low loading rate, criteria (17) and (18) would reproduce the quasi-static maximum stress criterion, as the special case. Simple checks of this kind are essential, because they serve as a basic verification supporting the validity of the generalization.

Both yield criteria above involve only one critical stress parameter, and they required a single incubation time parameter for their dynamic generalization. This will not be the case for failure criteria of brittle materials, where one would have to take into consideration that the strength can be very different under the tension and the compression. The simplest example is the maximum stress failure criterion:

$$\sigma_1 \le \sigma_{*,T} \text{ and } |\sigma_3| \le \sigma_{*,C}, \qquad \text{(Eq 19)}$$

where $\sigma_{*,T}$ and $\sigma_{*,C}$ are the tensile and the compressive strengths, and σ_1 and σ_3 are the maximum and the minimum principal stresses, respectively. There is no reason to expect that the material would have identical dynamic behavior under tension and compression, therefore, the generalization of the maximum stress criterion would require two incubation time parameters, and the dynamic failure criterion will become

$$\overline{\sigma}_{1,\Im_T} \le \sigma_{*,T} \text{ and } \left|\overline{\sigma}_{3,\Im_C}\right| \le \sigma_{*,C}, \qquad \text{(Eq 20)}$$

where $\Im_T$ and $\Im_C$ are the incubation times associated with the tensile and the compressive failures, respectively. To determine their values, two sets of dynamic characterization tests should be carried out, one under tension and one under compression.

The examples shown above are relatively simple cases of generalization, where averaging of stress invariants and the association between them and the failure modes is straightforward. It would not be the case for many other failure criteria, such as Mohr criterion in its implementation as was recently proposed in (Ref 19), and Raghava-Candell-Yeh (Ref 20) for isotropic materials, let alone for failure criteria for anisotropic materials, e.g., Tsai-Wu criterion (Ref 21). Their generalizations will be addressed in the future as separate accounts.

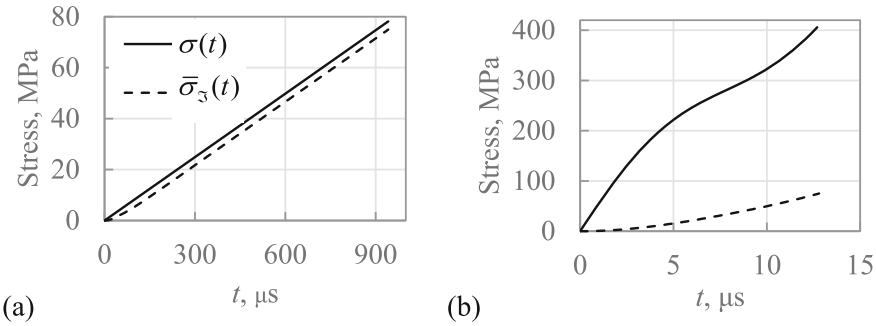

Fig. 6 Current and averaged stress time histories at (a) $\dot{\varepsilon} = 30\ \mathrm{s}^{-1}$, (b) $\dot{\varepsilon} = 10000\ \mathrm{s}^{-1}$

3.4 Verification of the Generalized Dynamic Failure Criteria

To verify the implementation of the generalized failure criteria, dynamic strength was calculated with the FE model over the wide range of strain rates and compared with its analytical expression (8) in Fig. 7. In the FE modeling, two criteria were used for the dynamic strength predictions as separate cases, one being the generalized von Mises criterion (17) and another the generalized maximum stress criterion (20).

The most striking feature of the comparison in Fig. 7 is that at strain rates above $\dot{\varepsilon} = 1000\ s^{-1}$ there is a non-negligible discrepancy both between the strengths predicted with the von Mises and the maximum stress criteria in the FE model, as well as between those obtained via FE modeling and the analytical solution (8). The reason behind this is the effects of inertia, manifested as the loss of linearity and loss of the uniaxial stress state, as was elaborated in subsection 3.1. As has been shown, at high strain rates the stress oscillations occur, and stress can deviate significantly from the idealized linear appearance that is assumed when deriving the analytical solution (8). This naturally results in value of strength, that is determined in the FE models as the value of stress invariant at the time when the failure criterion is satisfied, being different from the analytical solution. Similarly, the discrepancy between the generalized von Mises and maximum stress criteria predictions is due to the contribution of nonzero stress components σ_2 and σ_3. They are involved in calculation of von Mises averaged stress (16), while do not play any part when the maximum stress criterion is used as a failure condition.

Note that at strain rates below $1000\ s^{-1}$ the discrepancy between the strengths calculated using von Mises and maximum stress criteria vanishes. This serves as additional confirmation that the mismatch was due to loss of the uniaxial stress state. However, lack of perfect agreement between the FE results and analytical solution in this range of strain rates must be explained. This is caused by approximate calculation of the stress impulse at $t > \Im$ that was discussed in detail in subsection 3.1. Referring to Fig. 3(b), $\dot{\varepsilon} = 1000\ s^{-1}$ is effectively a cutoff value for the strain rate where times to failure are beginning to exceed $\Im$, which results in loss of accuracy of calculating the averaged stresses, or stress invariants.

Results in Fig. 7 verify the implementation of the generalized dynamic failure criteria for a simple type of loading. As has been detailed above, there are rational and logical reasons behind the discrepancies between dynamic strength predictions obtained using two independent methods, namely, the FE modeling and the analytical solution. This basic study provides an insight into true complexity of addressing the dynamic failure problem computationally, when the uniaxial loading of the isotropic material may not result in a uniaxial stress state. This, in fact, questions representativeness of the assumption of uniaxial stress state in SHPB testing. Both problems are certainly worthy of comprehensive investigation, but that would be beyond the scope of the present paper.

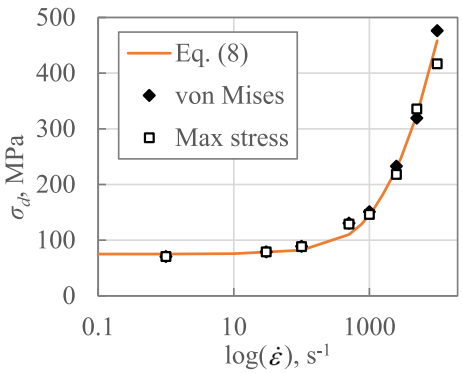

Fig. 7 Comparison of analytical and FE predictions of dynamic strength as a function of strain rate

4. Conclusions

Addressing a pressing demand for robust failure criteria that could be reliably used in computational modeling of dynamic failure of materials, method of generalizing the failure criteria has been proposed. It makes use of the previously established failure criterion that is stress impulse-based. A material property called incubation time of failure is involved in critical impulse definition. This property reflects the dynamic nature of the failure process.

Generalization was addressed from two perspectives. First, the implementation of the incubation time criterion as the computer code has been carried out, allowing failure predictions at arbitrary loading histories. Second, framework for deriving failure conditions applicable to a general stress state has been formulated. The underlying philosophy of the method is that any quasi-static stress invariant-based failure criterion can be generalized through an appropriate use of averaged stress invariants to its dynamic counterpart. The stress averaging procedure, which is key in implementation of this method, has also been established in the present paper. As an illustration of feasibility of the method, generalizations of von Mises, Tresca and maximum principal stress criteria have been carried out.

Open Access

This article is licensed under a Creative Commons Attribution 4.0 International License, which permits use, sharing, adaptation, distribution and reproduction in any medium or format, as long as you give appropriate credit to the original author(s) and the source, provide a link to the Creative Commons licence, and indicate if changes were made. The images or other third party material in this article are included in the article's Creative Commons licence, unless indicated otherwise in a credit line to the material. If material is not included in the article's Creative Commons licence and your intended use is not permitted by statutory regulation or exceeds the permitted use, you will need to obtain permission directly from the copyright holder. To view a copy of this licence, visit http://creativecommons.org/licenses/by/4.0/.

References

1. G.R. Johnson and W.H. Cook, Fracture Characteristics of three Metals Subjected to Various Strains, Strain Rates, Temperatures and Pressures, *Eng. Fract. Mech.*, 1985, **21**(1), p 31–48.
2. Abaqus Analysis User's Guide, Abaqus 2019 HTML Documentation. 2016
3. J.W. Swegle and D.E. Grady, Shock Viscosity and the Prediction of Shock Wave Rise Times, *J. Appl. Phys.*, 1985, **58**(2), p 692–701.

4. Johnson GR, Cook WH, A constitutive model and data for metals subjected to large strains, high strain rates and high temperatures, In *7th International Symposium on Ballistics*. 1983. p. 541–547
5. Yen C, Ballistic Impact Modeling of Composite Materials, In *International LS-DYNA Users Conference*. 2002: Dearborn, Michigan. p. 6.15–6.26
6. DATASHEET/PRIME™ 20LV - Epoxy Infusion System (v13), Gurit©, Editor. 2019
7. Pan Q, Multi-scale modelling and material characterisation of textile composites for aerospace applications. 2016, University of Nottingham
8. D.J. Frew, M.J. Forrestal, and W. Chen, Pulse Shaping Techniques for Testing Brittle Materials with a Split Hopkinson Pressure Bar, *Exp. Mech.*, 2002, **42**(1), p 93–106.
9. Y.V. Petrov, On 'Quantum' Nature of Dynamic Fracture of Brittle Media, *Doklady Academii Nauk SSSR*, 1991, **321**(1), p 66–68.
10. Y.V. Petrov, A.A. Gruzdkov, and V.A. Bratov, Structural-Temporal Theory of Fracture as a Multiscale Process, *Phys. Mesomech.*, 2012, **15**(3), p 232–237.
11. Y. Petrov, Fracture, Electric Breakdown and Phase Transformations under Impact Loading, *Proced. Mater. Sci.*, 2014, **3**, p 467–472.
12. A.A. Gruzdkov, E.V. Sitnikova, N.F. Morozov, and Y.V. Petrov, Thermal Effect in Dynamic Yielding and Fracture of Metals and Alloys, *Math. Mech. Solids*, 2009, **14**(1–2), p 72–87.
13. Y.V. Petrov, A.V. Cherkasov, and N.A. Kazarinov, Instability of Critical Characteristics of Crack Propagation, *Acta Mech.*, 2021, **232**(5), p 1997–2003.
14. Y.V. Petrov and E.N. Borodin, Relaxation Mechanism of Plastic Deformation and Its Justification Using the Example of the Sharp Yield Point Phenomenon in Whiskers, *Phys. Solid State*, 2015, **57**(2), p 353–359.
15. H. Nie, W. Ma, K. Wang, J. Ren, J. Cao, and W. Dang, A Review of Dynamic Multiaxial Experimental Techniques, *Rev. Sci. Instrum.*, 2020, **91**(11), p 111501.
16. Li S, Sitnikova E, Representative volume elements and unit cells: concepts, theory, applications and implementation. 2019: Elsevier
17. R. Gerlach, C.R. Siviour, N. Petrinic, and J. Wiegand, Experimental Characterisation and Constitutive Modelling of RTM-6 Resin Under Impact Loading, *Polymer*, 2008, **49**(11), p 2728–2737.
18. S. Zhao, Y.V. Petrov, and G.A. Volkov, The Modified Relaxation Plasticity Model and the Non-Monotonic Stress–Strain Diagram, *Int. J. Mech. Sci.*, 2023, **240**, p 107919.
19. S. Li, Rational Implementation of the Mohr Criterion in Its General form, *Int. J. Mech. Sci.*, 2024, **279**, p 109449.
20. R. Raghava, R.M. Caddell, and G.S.Y. Yeh, The Macroscopic Yield Behaviour of Polymers, *J. Mater. Sci.*, 1973, **8**, p 225–232.
21. S. Tsai and E. Wu, A General Theory of Strength for Anisotropic Materials, *J. Compos. Mater.*, 1971, **5**, p 58–80.

Publisher's Note Springer Nature remains neutral with regard to jurisdictional claims in published maps and institutional affiliations.